

- (4) 各種 HGF 発現ウイルスベクターの野生型ラットへの intrathecal injection による HGF 発現の検討：上記結果から AAV2-HGF, AAV4-HGF, HSV1-HGF について解析をすすめた。その結果、発現レベルは AAV4-HGF については他の2つのベクターに比較し低いものの、残りの2つのベクターについては広範囲脊髄においてほぼ同レベルで HGF 蛋白質を発現することが明らかとなった。
- (5) HGF 発現ウイルスベクターの ALS モデル動物への投与研究：現在進行中である。

D. 考察

これまでの私達の ALS モデル Tg マウスと神経特異的 HGF 発現 Tg マウスの交配研究の結果、HGF が運動ニューロンとグリア細胞の両方に作用することで ALS に対する治療効果をもつことを明らかにしてきた。しかし、このアプローチをヒトに適用することは難しい。ヒトへ適用可能な HGF の供給法としては、リコンビナント HGF 蛋白質の持続供給法が考えられ、もし成功すれば理想的である。この場合、広範囲の神経系に HGF 蛋白質を供給できる必要があるが、この問題は解決可能である。一方、HGF の遺伝子治療も可能性が高い。実際大阪大学附属病院において、血管性疾患 (ASO) に対する naked plasmid を用いた HGF 遺伝子治療が開始され、

現時点までの評価では問題となる副作用もなく治療効果が認められている。したがって、ALS に適した HGF 遺伝子治療法を開発できれば福音となる可能性が高い。ALS は ASO と異なり長期間かかり病態が完成するため、HGF を長期間神経系に供給する必要がある。この目的には、欧米で使用が検討されているアデノ随伴ウイルスベクター (AAV) および単純ヘルペス I 型ウイルスベクター (HSV1) 等の適用の可能性があり、今回その可能性を検討した。HGF を ALS で障害される広範囲な脊髄運動ニューロンに供給するという基準で評価した結果、検討した中では AAV2 および HSV1 が一番可能性が高いと考えられた。

E. 結論

ALS 治療に適切な遺伝子治療ベクターとして検討した中では AAV2-HGF と HSV1-HGF の2つが可能性をもつことが明らかとなった。

F. 研究発表

1. Isogawa K, Akiyoshi J, Kodama K, Matsushita H, Takahashi, Tsutsumi T, Funakoshi H, Nakamura T, Anxiolytic effect of hepatocyte growth factor infused into rat brain. *Neuropsychobiology* 51(1):34-38, 2004.
2. Date I, Takagi N, Takagi K, Kago T, Matsumoto K, Nakamura T, Takeo S. Hepatocyte growth factor improved learning and memory dysfunction of microsphere-embolized rats. *J Neurosci Res.* 78(3):442-5, 2004.
3. Date I, Takagi N, Takagi K, Kago T,

- Matsumoto K, Nakamura T, Takeo S. Hepatocyte growth factor attenuates cerebral ischemia-induced learning dysfunction. **Biochem Biophys Res Commun.** 319(4):1152-8, 2004.
4. Oshima K, Shimamura M, Mizuno S, Tamai K, Doi K, Morishita R, Nakamura T, Kubo T, Kaneda Y. Intrathecal injection of HVJ-E containing HGF gene to cerebrospinal fluid can prevent and ameliorate hearing impairment in rats. **FASEB J.** 18(1):212-4, 2004.
 5. Funakoshi H, Nakamura T. Hepatocyte growth factor: from diagnosis to clinical applications. **Clin Chim Acta.** 327:1-23 2003.
 6. Kato S, Funakoshi H, Nakamura T, Kato M, Nakano I, Hirano A, Ohama E. Expression of hepatocyte growth factor and c-Met in the anterior horn cells of the spinal cord in the patients with amyotrophic lateral sclerosis (ALS): immunohistochemical studies on sporadic ALS and familial ALS with superoxide dismutase 1 gene mutation. **Acta Neuropathol (Berl).** 106(2):112-20, 2003.
 7. 船越 洋、中村 敏一、肝細胞増殖因子 (HGF) は筋萎縮性側索硬化症 (ALS) の進行を遅らせる。神経治療学 Vol.20 No.5 : 533-540 2003.
 8. 船越 洋、中村 敏一、ALS と神経栄養因子—HGF による新しい治療法開発の可能性—。脳神経 55(10):841-845, 2003.

ALS ラットに対する肝細胞増殖因子（HGF）髄腔内投与による病態進行の抑制
および内在性神経前駆細胞の賦活の試み

分担研究者 青木 正志 東北大学病院神経内科助手

研究要旨 私たちは筋萎縮性側索硬化症（ALS）に対する新規治療法の開発のため、これまでに ALS の動物モデルの SOD1 トランスジェニック（Tg）ラットに対するヒトリコンビナント（hr）肝細胞増殖因子（HGF）の発症前髄腔内持続投与を行い、発症遅延の効果を報告した。今回は発症期からの HGF 投与によっても ALS ラットの死亡の遅延が確認され、臨床での効果が期待される。さらには HGF の脊髄前角運動神経細胞死抑制の機序として神経細胞の caspase 活性の抑制、内因性の XIAP 保持、EAAT2 の発現増加が明らかとなった。

ALS ラット脊髄における未分化な神経前駆細胞の増殖は、運動ニューロン脱落が進行した発症後期から末期になりはじめて有意なものとなる。このような細胞群を早期から賦活し組織修復に役立てることを目的として、再生誘導因子の1つである HGF の髄腔内投与を試みたところ、本モデルラット脊髄の新生細胞増殖の促進が確認された。現在、HGF により賦活された細胞群の形質と局在について検討中であるが、将来的に HGF をはじめとした外来性再生誘導因子の投与が新しい治療法開発につながる可能性がある。

分担研究者：青木正志

東北大学病院神経内科助手

研究協力者：石垣あや¹、割田 仁^{1,2}、永井真貴子¹、松本 有史^{1,7}、加藤昌昭^{1,3}、船越 洋⁴、加藤信介⁵、加藤雅子⁶、岡野栄之⁷、糸山泰人¹

¹東北大学大学院医学系研究科神経内科

²国立病院機構米沢病院神経内科

³国立病院機構宮城病院神経内科

⁴大阪大学大学院医学系研究科分子組織再生分野

⁵鳥取大学医学部附属脳幹性疾患研究施設脳神経病理部門、⁶病院病理部

⁷慶應義塾大学医学部生理学

A. 研究目的

系統的な運動ニューロン死を特徴とする神経変性疾患である ALS は致命的にもかかわらず有効な治療法が未だなく、これほど新規治療法開発が強く希求されている疾患はない。しかし、優性遺伝性 ALS の一部における Cu/Zn superoxide dismutase (SOD1) 遺伝子変異の発見から現在まで依然として病態には不明な点が多い。これまでに私たちは ALS の新しい動物モデルとしてヒト変異 SOD1 トランスジェニックラット（Tg ラット）を

確立した。従来のマウスモデルではなく、このラットモデルを用いることで髄腔内投与や細胞移植などの実験的治療を行うことがきわめて容易となった。

① ALS ラットに対する肝細胞増殖因子（HGF）髄腔内投与による病態進行抑制の試み

私たちはこれまでに、ALS の動物モデルの G93A SOD1 Tg ラットに対する発症前の 100 日齢からの hr HGF の髄腔内持続投与による腰髄運動神経細胞の脱落抑制と発症の遅延を報告してきた（平成 14 年度 研究報告書）。今回は hrHGF を発症期にあたる 115 日齢から G93A SOD1 Tg ラットの髄腔内に投与し、病態進行抑制効果の有無とその作用機序を検討した。

② HGF 髄腔内投与による内在性神経前駆細胞の賦活の試み

正常成体脊髄にも潜在的神経再生能があることが示されてきた近年、a) 外来性の細胞移植あるいは b) 内在性神経前駆細胞を利用した再生医療が脊髄の変性疾患である ALS の新規治療戦略として注目されている。また、近年までに神経前駆細胞

胞の増殖、分化、遊走、突起伸展を調節するさまざまな因子が報告されており、とくに *in vitro* ではこれらの“再生誘導”因子に関する研究が益々活発になされている。

我々は再生医療の開発を目的に内在性神経前駆細胞の解析を開始し、Tg ラット脊髄では運動ニューロン脱落前からグリア細胞新生 (gliogenesis) が認められるとともに、発症後期から末期に至ってようやく未分化な神経前駆細胞が増殖していることを昨年までに示した。本年度は Tg ラット脊髄に外来性再生誘導因子の一候補である肝細胞増殖因子 (HGF) を投与することで、内在性神経前駆細胞の賦活を試みた。

B. 研究方法

①平均発症時期頃の 115 日齢から hrHGF200 μ g/匹と、対照群として PBS をそれぞれメス G93A Tg ラット 8 匹ずつに 4 週間髄腔内持続投与し、死亡するまで経過を観察した。これとは別に検体採取用に 115 日齢からメス G93A SOD1 Tg ラットに hrHGF100 μ g/匹と、対照群として PBS をそれぞれ 2 週間髄腔内持続投与後腰髄を採取し、第 5 腰髄の免疫染色と前角運動神経細胞数の計測、ウェスタンブロットを行い、採取するまでの期間 foot print と体重の計測を行った。

②発症直前かつ脊髄運動ニューロン脱落開始直後の 18 週齢 (pre-symptomatic, Pre 期)、および発症後期にあたる 22 週齢 (symptomatic, Sym 期) のヒト H46R SOD1 Tg ラットに対して、ヒトリコンビナント HGF (総量 100 μ g/匹) を 2 週間にわたり浸透圧ポンプ (Alzet model 2002, 流量 0.5 μ L/時) によって髄腔内に持続投与した。vehicle としては人工髄液 (artificial cerebrospinal fluid, aCSF) を用いた。HGF 投与群と vehicle 投与群 (各群 n=4~5) いずれに対しても HGF 投与期間の後半 1 週間にチミジン類似体 5-bromo-2'-deoxyuridine (BrdU) を 1 日 1 回腹腔内投与 (50 mg/kg 体重) して新生細胞を標識した。2 週間の投与期間終了翌日に脊髄腰膨大部の灌流固定後凍結切片を作成して蛍光免疫組織化学的に解析した。一個体につき少なくとも 5 切片以上の多重切片を得て、一横断切片あたりの BrdU 陽性細胞数を計測、統計学的検討を加えた。

モデル動物の飼育・管理は当学動物実験ガイドラインを遵守した。

C. 研究結果

①平均発症は HGF 投与群が 126.8 \pm 13.1 日、対照群が 126.3 \pm 13.8 日 ($p=0.87455$) と有意差は認められなかった。平均死亡は HGF 投与群が 154.3 \pm 16.4 日、対照群が 143.25 \pm 17.0 日 ($p=0.02323$) と HGF 投与群が対照群より有意に遅延した。発症から死亡までの平均罹病期間が、HGF 投与群が 27.5 \pm 11.1 日間、対照群が 16.9 \pm 8.17 日間と、HGF 投与群では対照群の 62.7%の増大を示し、発症期の投与によっても HGF が Tg ラットの罹病期間を大幅に延長させることが示された。foot print と体重は、HGF 投与群が対照群よりも保たれ、両者とも 118 日齢で統計学的な有意差を認めた (foot print : 118 日齢 $p=0.0424$ 、体重 : 118 日齢 $p=0.0047$)。

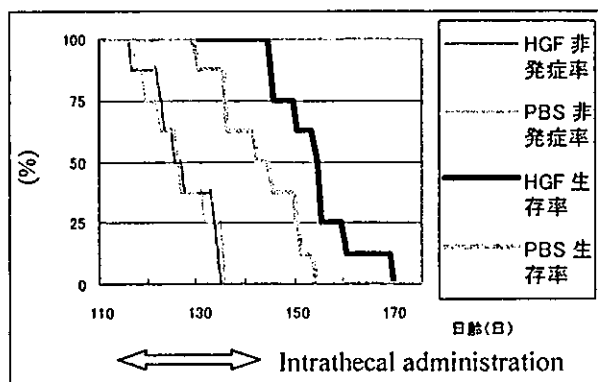


図1. 115日齢からのHGF投与による病態進行抑制効果

第 5 腰髄の前角運動神経細胞数は、HGF 投与群は平均 14.5 個、対照群は平均 8.33 個 ($p=0.02846$) と HGF 投与群の運動神経細胞数が対照群よりも有意に保持されていた。免疫染色の結果は、活性型の HGF 受容体であるリン酸化 C-met は HGF 投与群のほうが強く染色された。active caspase-3 および active caspase-9 は対照群のほうが強く染色され HGF 投与群では抑制されていた。

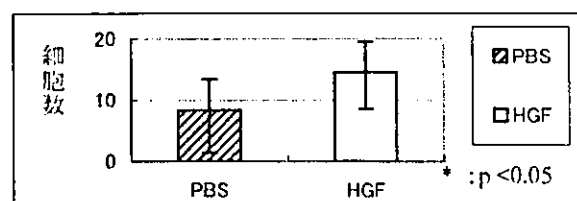


図2. 運動神経細胞数 (第5腰髄前角)

ウェスタンブロット (図3) では各バンドの

density を定量解析し、内部標準との比の平均値を算出した。HGF 投与群が対照群よりも caspase-3、9 のバンドが減弱し、caspase-3 では有意差を認めた (pro-caspase-9 : $p=0.694$ 、active caspase-9 : $p=0.2364$ 、pro-caspase-3 : $p=0.0031$ 、active caspase-3 : 0.0154)。GFAP のバンドは HGF 投与群と対照群とほぼ同様だった。一方、XIAP、EAAT2 のバンドは HGF 投与群の方が対照群よりも増強しており (XIAP : $p=0.0099$ 、EAAT2 : 0.0417)、特に EAAT2 では HGF 投与群が正常ラットよりもバンドが増強していた。

② Pre 期と Sym 期の vehicle 投与群だけを比較すると、病期の進行に伴い BrdU 陽性細胞数が増

加していた。これに対して、Pre 期の HGF 投与群では vehicle 群に比較して BrdU 陽性細胞数がさらに増加する傾向が認められた (有意差なし)。一方、Sym 期の HGF 投与群では vehicle 群に比較して優位に BrdU 陽性細胞数が増加していた (図 4)。

現在、これらの BrdU 陽性細胞の形質と局在を他の選択的細胞マーカーとの多重免疫組織化学を用いて解析中である。

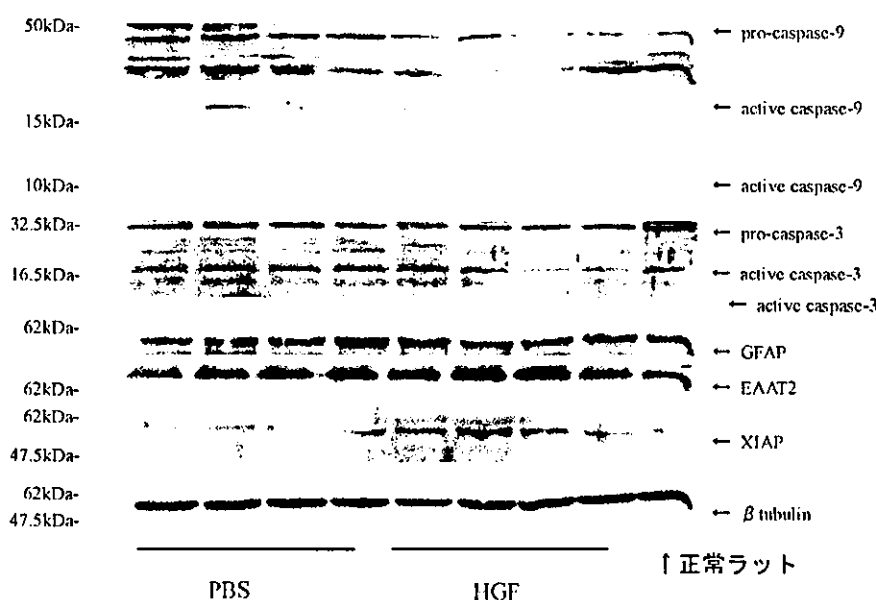


図3. ウェスタンブロット (腰髄)

D. 考察

発症時期からの投与により罹病期間延長効果が得られたことから、臨床において発症後 ALS と診断されてから ALS 患者に HGF を投与開始しても、病態進行抑制効果が期待できる可能性が示された。このことは、臨床への応用という点に関して、注目すべき結果と考える。

HGF 投与による病態進行抑制の機序として、caspase cascade の主な実行因子とされている、caspase-3、9 の抑制効果を認めたことから caspase cascade、またはその上流の細胞死機序を抑制することが示唆された。EAAT2 が発現増加し XIAP が保持されたことから、細胞保護機能の維持・増強が示され、またアストロサイトなどの神経細胞以外の神経組織構成細胞にも HGF が作用

することが示された。

HGF 髄腔内投与による神経前駆細胞の賦活に関しては HGF 投与によって病態下脊髄で増加しつつある新生細胞をさらに増加させることが示された。近年、*in vitro* で HGF が neurosphere 形成細胞の増殖、ニューロンへの分化促進といった再生誘導能を示すことが報告されている (Kokuzawa J, et al. 2003)。本研究により *in vivo* でも、HGF が神経前駆細胞を賦活させる可能性が示された。しかし、HGF は多様な機能をもつサイトカインであることから、神経前駆細胞への直接賦活効果だけでなく、運動ニューロン死抑制効果、astrocyte 機能改善効果を介した間接効果もまた想定される (Sun W, Funakoshi H, et al. 2002)。したがって、HGF が増殖促進した細胞群についての解析

に加え、HGF 受容体 c-Met の発現や前駆細胞以外の細胞種、細胞外環境への効果についても検討を要する。

また、運動ニューロン脱落開始直後 (Pre 期) よりは、より進行期 (Sym 期) に HGF を投与する方が新生細胞増加促進の度合いが大きいことが示された。このことは、運動ニューロン脱落が一定レベル以上に生じた環境の方がより新生細胞の増加を許容しやすいという可能性を示唆し、細胞外環境 (液性因子等) の関与が想定される。

最後に、髄腔内投与法は主病変部位が脊髄に系統的に存在しかつ血液脳関門が障害となる HGF のようなペプチド因子投与の場合、病変部位に効率よく到達させる優れた投与方法であることがあらためて確認された。

E. 結論

発症時期からの投与により罹病期間延長効果を示した HGF は、臨床での治療効果が大きいと期待できる。その作用機序として細胞死抑制、細胞保護機能の維持・増強が確認された。

さらには HGF 髄腔内投与が脊髄において新生細胞を増加させることが示された。今後は HGF の至適用量や投与時期の検討、他の再生誘導因子と組み合わせ投与、細胞移植、治療的遺伝子導入などとの組み合わせを検討することで、内在性神経前駆細胞を賦活するような新規治療法につながる可能性がある。

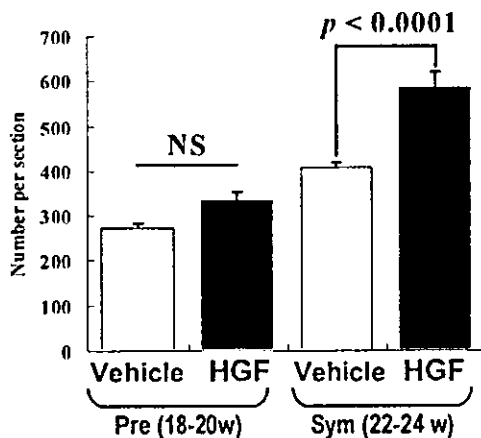


図 4. 腰髄 BrdU 陽性細胞数の変化 (本文参照)

F. 健康危険情報

特に無し

G. 研究発表

1. 論文発表

- 1) Miyazaki K, Fujita T, Ozaki T, Kato C, Kurose Y, Sakamoto M, Kato S, Goto T, Itoyama Y, Aoki M, Nakagawara A: NEDL1, a novel ubiquitin-protein isopeptide ligase for dishevelled-1, targets mutant superoxide dismutase-1. *J Biol Chem* 279: 11327-11335, 2004
- 2) Kato S, Saeki Y, Aoki M, Nagai M, Ishigaki A, Itoyama Y, Kato M, Asayama K, Awaya A, Hirano A, Ohama E: Histological evidence of redox system breakdown caused by superoxide dismutase 1 (SOD1) aggregation is common to SOD1-mutated motor neurons in humans and animal models. *Acta Neuropathol* 107: 149-158, 2004
- 3) Yasuda H, Ebihara S, Yamaya M, Asada M, Sasaki H, Aoki M: Increased arterial carboxyhaemoglobin concentrations in patients with sporadic amyotrophic lateral sclerosis. *J Neurol Neurosurg Psychiatry* 75: 1076-1077, 2004
- 4) Suzuki N, Aoki M, Takahashi T, Takano D, Asano M, Shiga Y, Onodera Y, Tateyama M, Itoyama Y: Novel dysferlin mutations and characteristic muscle atrophy in late-onset Miyoshi myopathy. *Muscle Nerve* 29: 721-723, 2004

2. 学会発表

第 45 回日本神経学会総会 2004.5 東京

H. 知的財産権の出願・登録状況

ラットを用いた ALS モデル (出願済)

研究成果の刊行に関する一覧表

研究成果の刊行に関する一覧表

原著論文

著者	論文タイトル	掲載誌名	巻		出版年
			ページ		
Miyazaki K, Fujita T, Ozaki T, Kato C, Kurose Y, Sakamoto M, Kato S, Goto T, Itoyama Y, Aoki M, Nakagawara A	NEDL1, a novel ubiquitin-protein isopeptide ligase for dishevelled-1, targets mutant superoxide dismutase-1	J Biol Chem	279	11327-11335	2004
Kato S, Saeki Y, Aoki M, Nagai M, Ishigaki A, Itoyama Y, Kato M, Asayama K, Awaya A, Hirano A, Ohama E	Histological evidence of redox system breakdown caused by superoxide dismutase 1 (SOD1) aggregation is common to SOD1-mutated motor neurons in humans and animal models	Acta Neuropathol	107	149-158	2004
Yasuda H, Ebihara S, Yamaya M, Asada M, Sasaki H, Aoki M	Increased arterial carboxyhaemoglobin concentrations in patients with sporadic amyotrophic lateral sclerosis	J Neurol Neurosurg Psychiatry	75	1076-1077	2004
Suzuki N, Aoki M, Takahashi T, Takano D, Asano M, Shiga Y, Onodera Y, Tateyama M, Itoyama Y	Novel dysferlin mutations and characteristic muscle atrophy in late-onset Miyoshi myopathy	Muscle Nerve	29	721-723	2004
Nagashima T, Chuma T, Mano Y, Goto Y, Hayashi YK, Minami N, Nishino I, Nonaka I, Takahashi T, Sawa H, Aoki M, Nagashima K	Dysferlinopathy associated with rigid spine syndrome	Neuropath	24	341-6	2004
Suzuki N, Aoki M, Hinuma Y, Takahashi T, Onodera Y, Ishigaki A, Kato M, Warita H, Tateyama M, Itoyama Y	Expression profiling with progression of dystrophic change in dysferlin-deficient mice (SJL)	Neurosci Res	in press		
Fujiwara N, Miyamoto Y, Ogasahara K, Takahashi M, Ikegami T, Takamiya R, Suzuki K, and Taniguchi N.	Different Immunoreactivity against Monoclonal Antibodies between Wild-type and Mutant Copper/Zinc Superoxide Dismutase Linked to Amyotrophic Lateral Sclerosis	J. Biol. Chem.	280	5061-5070	2005

著者	論文タイトル	掲載誌名	巻		出版年
			ページ		
Takamiya R., Takahashi M., Park Y.S. Tawara Y., Fujiwara N., Miyamoto Y., Gu J., Suzuki K. and Taniguchi N.	Overexpression of Mutated Cu,Zn-SOD in Neuroblastoma Cells Results in Cytoskeletal Change	Am. J. Physiol. Cell Physiol	288	C253-259	2005
Hanamoto T, Ozaki T, Furuya K, Hosoda M, Hayashi S, Nakanishi M, Yamamoto H, Kikuchi H, Todo S, Nakagawara A.	Identification of protein kinase A catalytic subunit (PKA-C) as a novel binding partner of p73 and regulation of p73 function.	J. Biol. Chem.	in press		
Ohira M, Oba S, Nakamura Y, Hirata T, Ishii S, Nakagawara A.	A review of DNA microarray analysis of human neuroblastomas.	Cancer Lett.	in press		
Lin L, Ozaki T, Takada Y, Kageyama H, Nakamura Y, Hata A, Zhang J-H, Simonds W, Nakagawara A, Koseki H.	Topors, a p53 and topoisomerase I-binding RING finger protein, is a co-activator of p53 in growth suppression induced by DNA damage.	Oncogene	in press		
Ozaki T, Hosoda M, Miyazaki K, Hayashi S, Watanabe K, Nakagawa T, Nakagawara A.	Functional implication of p73 protein stability in neuronal cell survival and death.	Cancer Lett.	in press		
Kato C, Hanamoto T, Nakagawara A.	Protein stability and function of p73 are modulated by a physical interaction with RanBPM in mammalian cultured cells.	Oncogene	24	938-944	2005
Abe M, Ohira M, Kaneda A, Yagi Y, Yamamoto S, Kitano Y, Takato T, Nakagawara A, Ushijima T.	CpG island methylator phenotype is a strong determinant of poor prognosis in neuroblastomas.	Cancer Res.	65	828-834	2005
Nakagawara A, Ohira M.	Comprehensive genomics linking between neural development and cancer: Neuroblastoma as a model. In Special Issue: Neural development and cancer.	Cancer Lett.	204	23-224	2004
Miyazaki K, Fujita T, Ozaki T, Kato C, Kurose Y, Sakamoto M, Kato S, Goto T, Itoyama Y, Aoki M, Nakagawara A.	NEDL1, a novel ubiquitin-protein isopeptide ligase for Dishevelled-1, targets mutant superoxide dismutase-1.	J. Biol. Chem.	279	11327-11335	2004

著者	論文タイトル	掲載誌名	巻		出版年
			ページ		
Hamano S, Ohira M, Isogai E, Nakada K, Nakagawara A.	Identification of novel human neuronal leucine-rich repeat (hNLRR) family genes and inverse association of expression of Nbla10449/hNLRR-1 and Nbla10677/hNLRR-3 with the prognosis of primary neuroblastomas.	Int. J. Oncol.	24	1457-1466	2004
Ohtori S, Isogai E, Hasue F, Ozaki T, Nakamura Y, Nakagawara A, Kosoki H, Yuasa S, Hanaoka E, Shinbo J, Yamamoto T, Chiba H, Yamazaki M, Moriya H, Sakiyama S.	Reduced inflammatory pain in mice deficient in the differential screening-selected gene abrrative in neuroblastoma.	Mol. Ccell. Neurosci.	245	504-514	2004
K, Yu L, Ōgi T, Takenaga K, Shishikura T, Nakagawara A, Sakiyama S, Tagawa M and O-Wang J.	Elevated expression of DNA polymerase k in human lung cancer is associated with p53 inactivation: negative regulation of POLK promoter activity by p53.	Int. J. Oncol.	25	161-165	2004
Ando K, Ozaki T, Yamamoto H, Furuya K, Hosoda M, Hayashi S, Fukuzawa M, Nakagawara A.	Polo-like kinase 1 (Plk1) inhibits p53 function by physical interaction and phosphorylation.	J. Biol. Chem.	279	25549-25561	2004
Hiyama E, Yamaoka H, Matsunaga T, Hayashi Y, Ando H, Suita S, Horie H, Kaneko M, Sasaki F, Hashizume K, Nakagawara A, Ohnuma N, Yokoyama T.	High expression of telomerase is an independent prognostic indicator of poor outcome in hepatoblastoma.	Br. J. Cancer	291	972-979	2004
Yamada S, Ohira M, Horie H, Ando K, Takayasu H, Suzuki Y, Sugano S, Matsunaga T, Hiyama E, Hayashi Y, Watanabe Y, Suita S, Kaneko M, Sasaki F, Hashizume K, Ohnuma N, Nakagawara A.	Expression profiling and differential screening between hepatoblastomas and the corresponding normal livers: Identification of high expression of the Plk1 oncogene as a poor-prognostic indicator of hepatoblastomas.	Oncogene	23	5901-5911	2004
Takahashi M, Ozaki T, Todo S, Nakagawara A.	Decreased expression of the candidate tumor suppressor gene ING1 is associated with poor prognosis in advanced neuroblastomas.	Oncol Rep.	12	811-816	2004

著者	論文タイトル	掲載誌名	巻		出版年
			ページ		
Kato C, Miyazaki K, Nakagawa A, Ohira M, Nakamura Y, Ozaki T, Imai T, Nakagawara A.	Low expression of human tubulin tyrosine ligase and suppressed tubulin tyrosination/detyrosination cycle are associated with impaired neuronal differentiation in neuroblastomas with poor prognosis.	Int. J. Cancer	112	365-375	2004
Isogawa K, Akiyoshi J, Kodama K, Matsushita H, Takahashi, Tsutsumi T, Funakoshi H, Nakamura T.	Anxiolytic effect of hepatocyte growth factor infused into rat brain.	Neuropsychobiology	51(1)	34-38	2004
Date I, Takagi N, Takagi K, Kago T, Matsumoto K, Nakamura T, Takeo S.	Hepatocyte growth factor attenuates cerebral ischemia-induced learning dysfunction.	Biochem Biophys Res Commun.	319(4)	1152-8	2004
Date I, Takagi N, Takagi K, Kago T, Matsumoto K, Nakamura T, Takeo S.	Hepatocyte growth factor improved learning and memory dysfunction of microsphere-embolized rats.	J Neurosci Res.	78(3)	442-5	2004
Oshima K, Shimamura M, Mizuno S, Tamai K, Doi K, Morishita R, Nakamura T, Kubo T, Kameda Y.	Intrathecal injection of HVJ-E containing HGF gene to cerebrospinal fluid can prevent and ameliorate hearing impairment in rats.	FASEB J.	18(1)	212-4	2004

書籍

著者	論文タイトル	書籍全体の 編集者	書籍名	出版社	巻		出版年
					ページ	ページ	
青木正志	新世代の筋萎縮性側索硬化症 (ALS) の動物モデル		細胞工学		23 838-841		2004
青木正志、永井真貴子、 石垣あや、糸山泰人	神経栄養因子HGFの髄腔内投与によるALS治療法の開発		最新医学		59 87-93		2004
Nakagawara A.	Molecular and developmental biology of neuroblastoma	S. Cohn & N-K. Cheung	Neuroblastoma	Springer-Verlag, Heidelberg	in press		2005
Nakagawara A.	In NGF and Related Molecules in Health and Disease: Neural crest development and neuroblastoma: the genetic and biological link.	Luigi Aloe & Laura Calza	Progress in Brain Research	Elservier Science Publisher	146 233-242		2004

NEDL1, a Novel Ubiquitin-protein Isopeptide Ligase for Dishevelled-1, Targets Mutant Superoxide Dismutase-1*

Received for publication, November 12, 2003, and in revised form, December 16, 2003
Published, JBC Papers in Press, December 18, 2003, DOI 10.1074/jbc.M312389200

Kou Miyazaki†, Tomoyuki Fujita†, Toshinori Ozaki†, Chiaki Kato‡, Yuka Kurose‡, Maya Sakamoto‡, Shinsuke Kato§, Takeshi Goto¶, Yasuto Itoyama||, Masashi Aoki||, and Akira Nakagawara†**

From the †Division of Biochemistry, Chiba Cancer Center Research Institute, Chiba 260-8717, Japan, the ‡Division of Neuropathology, Institute of Neurological Sciences, Faculty of Medicine, Tottori University, Yonago 683-8504, Japan, ¶Hisamitsu Pharmaceutical Company Incorporated, Tokyo 100-622, Japan, and the ||Department of Neurology, Tohoku University School of Medicine, Sendai 980-8574, Japan

Approximately 20% of familial amyotrophic lateral sclerosis (FALS) arises from germ-line mutations in the superoxide dismutase-1 (SOD1) gene. However, the molecular mechanisms underlying the process have been elusive. Here, we show that a neuronal homologous to E6AP carboxyl terminus (HECT)-type ubiquitin-protein isopeptide ligase (NEDL1) physically binds translocon-associated protein- δ and also binds and ubiquitinates mutant (but not wild-type) SOD1 proportionately to the disease severity caused by that particular mutant. Immunohistochemically, NEDL1 is present in the central region of the Lewy body-like hyaline inclusions in the spinal cord ventral horn motor neurons of both FALS patients and mutant SOD1 transgenic mice. Two-hybrid screening for the physiological targets of NEDL1 has identified Dishevelled-1, one of the key transducers in the Wnt signaling pathway. Mutant SOD1 also interacted with Dishevelled-1 in the presence of NEDL1 and caused its dysfunction. Thus, our results suggest that an adverse interaction among misfolded SOD1, NEDL1, translocon-associated protein- δ , and Dishevelled-1 forms a ubiquitinated protein complex that is included in potentially cytotoxic protein aggregates and that mutually affects their functions, leading to motor neuron death in FALS.

loss of motor neurons in the spinal cord, brain stem, and motor cortex. The sporadic and familial forms of the disease have similar clinical and pathological features. About 10% of ALS cases are familial, and mutation of superoxide dismutase-1 (SOD1) is found in 20% of familial ALS (FALS) patients (1, 2). Mice that express mutant SOD1 transgenes develop an age-dependent ALS phenotype independent of levels of dismutase activity, suggesting that FALS pathology is because of a toxic gain of function in SOD1 and that the abnormal protein structure of mutant SOD1 is critical in the pathogenesis of motor neuron death (3–6). Recently, proteasome expression and activity have been reported to decrease with age in the spinal cord (7, 8). Furthermore, mutant SOD1 turns over more rapidly than wild-type SOD1, and an inhibitor of proteasome action inhibits this turnover and thus selectively increases the steady-state level of mutant SOD1 (8). These results suggest the involvement of the ubiquitin-proteasome function in the cause of FALS. However, the biochemical nature of this gain-of-function mutation in SOD1 and the mechanism by which SOD1 mutations cause the degeneration of motor neurons have remained elusive.

We show here the identification of a novel HECT-type ubiquitin-protein isopeptide ligase (E3), NEDL1, which is expressed in neuronal tissues, including the spinal cord, and selectively binds to and ubiquitinates mutant (but not wild-type) SOD1. NEDL1 is physically associated with translocon-associated protein- δ (TRAP- δ), one of the endoplasmic reticulum (ER) translocon components that has previously been reported to bind mutant SOD1 (9, 10). Both NEDL1 and TRAP- δ form a complex with mutant SOD1, with the binding intensity among these proteins being roughly proportionate to the rapidity of progression of the associated FALS phenotype. Immunohistochemical study has shown that NEDL1 is positive in the Lewy body-like hyaline inclusions in the spinal cord motor neurons of both FALS patients and mutant SOD1 transgenic mice. We have also found that NEDL1 targets Dishevelled-1 (Dvl1) for ubiquitination-mediated degradation and that mutant (but not wild-type) SOD1 affects the function of Dvl1. Our observations suggest that NEDL1 is a quality control E3 that recognizes mutant SOD1 to form a tight complex with the physiological targets of NEDL1 in motor neurons of FALS patients.

EXPERIMENTAL PROCEDURES

Cell Culture and Transfection—Human neuroblastoma-derived cells were grown in RPMI 1640 medium supplemented with 10% heat-inactivated fetal bovine serum, 100 units/ml penicillin, and 100 μ g/ml streptomycin. COS-7 and Neuro2a cells were maintained in Dulbecco's modified Eagle's medium supplemented with 10% heat-inactivated fe-

Amyotrophic lateral sclerosis (ALS)¹ is a progressive, fatal, neurodegenerative disease that is characterized by selective

* This work was supported in part by Hisamitsu Pharmaceutical Co. Inc. (to A. N.), by grants from the Ministry of Health, Labor, and Welfare of Japan (to A. N. and Y. I.), and by grants from the Ministry of Education, Culture, Sports, Science, and Technology of Japan (to A. N., Y. I., and M. A.). The costs of publication of this article were defrayed in part by the payment of page charges. This article must therefore be hereby marked "advertisement" in accordance with 18 U.S.C. Section 1734 solely to indicate this fact.

The nucleotide sequence(s) reported in this paper has been submitted to the GenBank™/EBI Data Bank with accession number(s) AB048365 (Nbla0078 and human NEDL1), AB002320 (KIAA0322), and AB083710 (mouse Nedd1).

** To whom correspondence should be addressed: Div. of Biochemistry, Chiba Cancer Center Research Inst., 666-2 Nitona, Chuoh-ku, Chiba 260-8717, Japan. Tel.: 81-43-264-5431; Fax: 81-43-265-4459; E-mail: akiranak@chiba-ceri.chuo.chiba.jp.

¹ The abbreviations used are: ALS, amyotrophic lateral sclerosis; FALS, familial amyotrophic lateral sclerosis; SOD1, superoxide dismutase-1; E3, ubiquitin-protein isopeptide ligase; NEDL1, NEDD4-like ubiquitin-protein ligase-1; TRAP- δ , translocon-associated protein- δ ; ER, endoplasmic reticulum; Dvl1, Dishevelled-1; RT, reverse transcription; LBHI, Lewy body-like hyaline inclusion; JNK, c-Jun N-terminal kinase; HECT domain, homologous to E6AP carboxyl-terminus.

tal bovine serum, 100 units/ml penicillin, and 100 µg/ml streptomycin. All cells were maintained in a humidified 37 °C incubator with 5% CO₂. All transfections were carried out with LipofectAMINE Plus transfection reagent (Invitrogen) according to the manufacturer's instructions. In some experiments, transfected cells were treated with MG-132 for 30 min at a final concentration of 40 µM.

RNA Analysis—A human multiple tissue mRNA blot and a fetal human multiple mRNA blot (Invitrogen) were hybridized with a ³²P-labeled ApaI-ScaI restriction fragment of *NEDL1* cDNA under standard conditions. For reverse transcription (RT)-PCR analysis, cDNA derived from adult human neural system (BioChain Institute, Hayward, CA) was subjected to PCR amplification using the following primers: *NEDL1*, 5'-CCGATTTGAGATCACTTCTCC-3' (sense) and 5'-CCGCTTTCCATCAGGTTGTT-3' (antisense); and glyceraldehyde-3-phosphate dehydrogenase, 5'-ACCTGACCTGCCGTCTAGAA-3' (sense) and 5'-TCCACCACCCTGTTGCTGTA-3' (antisense). The amplified products were separated by electrophoresis on a 1.5% agarose gel and visualized by ethidium bromide post-staining. Amplification of glyceraldehyde-3-phosphate dehydrogenase was used as an internal control.

In Vitro Ubiquitination Assays—*In vitro* ubiquitination assays were performed as follows. Reaction mixtures containing 0.5 µg of purified glutathione *S*-transferase fusion proteins, 0.25 µg of yeast ubiquitin-activating enzyme (*E1*) (BostonBiochem, Cambridge, MA), 1 µl of crude lysates from *Escherichia coli* expressing ubiquitin carrier proteins (*E2*), and 10 µg of bovine ubiquitin (Sigma) were incubated in 250 mM Tris-HCl (pH 7.6), 1.2 M NaCl, 50 mM ATP, 10 mM MgCl₂, and 30 mM dithiothreitol. Reactions were terminated after 2 h at 30 °C by the addition of SDS sample buffer. Samples were resolved by SDS-PAGE, transferred to membranes, and immunoblotted with anti-ubiquitin monoclonal antibody 1B3 (Medical & Biological Laboratories, Nagoya, Japan).

Immunofluorescence Staining—Cells grown on coverslips were processed for immunofluorescence. Briefly, cells were fixed in 3.7% formaldehyde, permeabilized in 0.2% Triton X-100, and finally incubated with anti-NEDL1 antibody (diluted 1:100). The primary antibody was detected with fluorescein isothiocyanate-conjugated goat anti-rabbit IgG (diluted 1:500; Jackson ImmunoResearch Laboratories, Inc., West Grove, PA). Images were taken using an Olympus confocal microscopy system.

Yeast Two-hybrid Screening—Yeast two-hybrid screening was performed using the Gal4-based Matchmaker two-hybrid system with the cDNA libraries derived from fetal human brain (first screening) and adult human brain (second screening) (Clontech, Palo Alto, CA). *Saccharomyces cerevisiae* CG1945 cells were transformed with pAS2-1-NEDL1-1 (amino acids 757–1114; first screening) or pAS2-1-NEDL1-2 (amino acids 332–1448; second screening), which did not activate the transcription of *lacZ* alone. The transformants were subsequently transformed with the cDNA library, and the *lacZ*-positive colonies were selected. The plasmid DNAs were extracted from these positive colonies, and their nucleotide sequences were determined.

Immunoprecipitation and Western Blot Analysis—Anti-NEDL1 and anti-TRAP-δ polyclonal antibodies were raised in rabbits against an NEDL1 oligopeptide (amino acids 460–482) and a TRAP-δ oligopeptide (amino acids 93–126), respectively. For immunoprecipitation, COS-7 or Neuro2a cells were cotransfected with the expression plasmids in various combinations and lysed 48 h later in 10 mM Tris-HCl (pH 7.8), 150 mM NaCl, 1% Nonidet P-40, 1 mM EDTA, and 1 mM phenylmethylsulfonyl fluoride supplemented with protease inhibitor mixture (Sigma). Whole cell lysates were immunoprecipitated with anti-NEDL1, anti-FLAG (M2; Sigma), or anti-Myc (9B11; Cell Signaling Technology, Beverly, MA) antibody. Immune complexes were recovered on protein G-Sepharose beads, eluted by boiling in Laemmli sample buffer, electrophoresed on SDS-polyacrylamide gel, and then transferred to a polyvinylidene difluoride membrane (Immobilon, Millipore Corp., Bedford, MA) by electroblotting. For ubiquitination experiments, cell lysis was performed in radioimmune precipitation assay buffer (10 mM Tris-HCl (pH 7.4), 150 mM NaCl, 1% Nonidet P-40, 0.1% sodium deoxycholate, 0.1% SDS, and 1 mM EDTA), followed by strong sonication and freeze-thaw. The membrane was probed with the indicated primary antibodies and then incubated with the appropriate secondary antibodies labeled with horseradish peroxidase (Jackson ImmunoResearch Laboratories, Inc. and Southern Biotechnology Associates, Inc., Birmingham, AL). Immunoreactive bands were detected by the enhanced chemiluminescence technique (ECL, Amersham Biosciences). For the detection of c-Jun phosphorylation, we used anti-c-Jun (sc-45, Santa Cruz Biotechnology, Santa Cruz, CA) or anti-phospho-Ser⁶³ c-Jun (Cell Signaling Technology) antibody.

Cloning of Human NEDL1 cDNA—A forward primer (5'-GGTTTT-

TAGGCTGGCCGCC-3') and a reverse primer (5'-CAATGAGGTA-CATGCCAATCC-3') were used to amplify the 5'-part of the *NEDL1* cDNA using cDNA libraries derived from human neuroblastoma and fetal human brain (Stratagene, La Jolla, CA) as templates. The full-length human *NEDL1* cDNA was generated by fusion of the PCR-amplified fragment (nucleotides +1 to +68, where position +1 represents the translation initiation site) and the *KIAA0322* cDNA (a gift from T. Nagase, Kazusa DNA Institute). Gel electrophoresis and Western blot analysis were carried out as described above.

Expression Constructs—The mammalian expression plasmids for hemagglutinin-tagged and His₆-tagged ubiquitin were kind gifts of D. Bohmann. The full-length *NEDL1* cDNA was inserted into the mammalian expression plasmid pEF1/His (Invitrogen) or pIRESpuro2 (Clontech). cDNAs encoding wild-type and mutant forms of SOD1 were fused to the FLAG or Myc epitope tag sequence at their C termini and subcloned into pIRESpuro2. Similarly, the FLAG or Myc epitope tag sequence was attached to the C terminus of TRAP-δ. Also similarly, the FLAG or Myc epitope tag sequence was attached to the N terminus of Dvl1. Coding sequences were verified by automated DNA sequencing.

Protein Stability Experiments—Neuro2a cells were transfected with the expression plasmid for the wild-type or mutant form of SOD1 with or without the *NEDL1* expression plasmid. Twenty-four hours after transfection, cycloheximide (50 µg/ml) was added to the culture medium, and the cells were harvested at the indicated time points by lysis in radioimmune precipitation assay buffer. The protein concentrations were determined using the Bradford protein assay system (Bio-Rad) according to the instructions of the manufacturer.

Immunohistochemistry—The immunohistochemical studies were performed as described previously using affinity-purified rabbit anti-NEDL1 antibody (11). Patient tissues were obtained at autopsy from two FALS siblings from a Japanese family. The clinical course of the sister, who died at age 46, was 18 months (case 1), and that of the brother, who died at age 65, was 11 years (case 2) (11). The *SOD1* gene was mutated with a 2-bp deletion at codon 126 (11, 12). Normal spinal cord tissues were obtained from three neurologically and neuropathologically normal individuals. The same study was performed on spinal cord tissues from three normal rats and a transgenic ALS rat carrying a mutant allele of the human *SOD1* gene (H46R) (13). These mice were killed at 180 days. As a negative control, some sections were incubated with anti-NEDL1 antibody that had been pre-absorbed with an excess of NEDL1 antigen. Bound antibodies were visualized by the avidin-biotin-immunoperoxidase complex method.

RESULTS

Cloning and Expression of the NEDL1 E3 Gene—To detect novel molecules that are important in regulating neuronal programmed cell death, we constructed oligo-capping cDNA libraries from a mixture of three fresh human neuroblastoma tissues (stages 1 and 2) that were undergoing gradual spontaneous regression, probably by neuronal apoptosis (14). Screening of 1152 novel genes by RT-PCR revealed that 194 genes were expressed differentially in regressing neuroblastomas with favorable prognosis and in aggressive tumors with poor prognosis. Among these genes, we found a partial cDNA sequence with an HECT-like domain (*Nbla0078*) that partially matched the *KIAA0322* gene. Because *KIAA0322* lacks a 5'-coding region, we used a genome-based PCR procedure to clone the corresponding full-length cDNA. This is predicted to encode a protein product of 1585 amino acids with homology to NEDD4 E3 (15, 16), which includes a C2 domain at the N-terminal region supposed to mediate its membrane localization in a calcium-dependent manner, two WW motifs important for protein-protein interaction through binding to specific proline-rich clusters, and a conserved catalytic HECT domain at the C terminus (Fig. 1A). We named this novel ligase, which mapped to chromosome 7p13, NEDL1 (*NEDD4*-like ubiquitin-protein ligase-1). We also cloned the mouse counterpart of *NEDL1* cDNA, whose amino acid sequence is 78% identical to the human sequence. Tissue-specific expression of *NEDL1* mRNA of ~10 and 7 kb in size was observed, with predominant expression in adult and fetal brains as examined by Northern blot analysis (Fig. 1B). Its

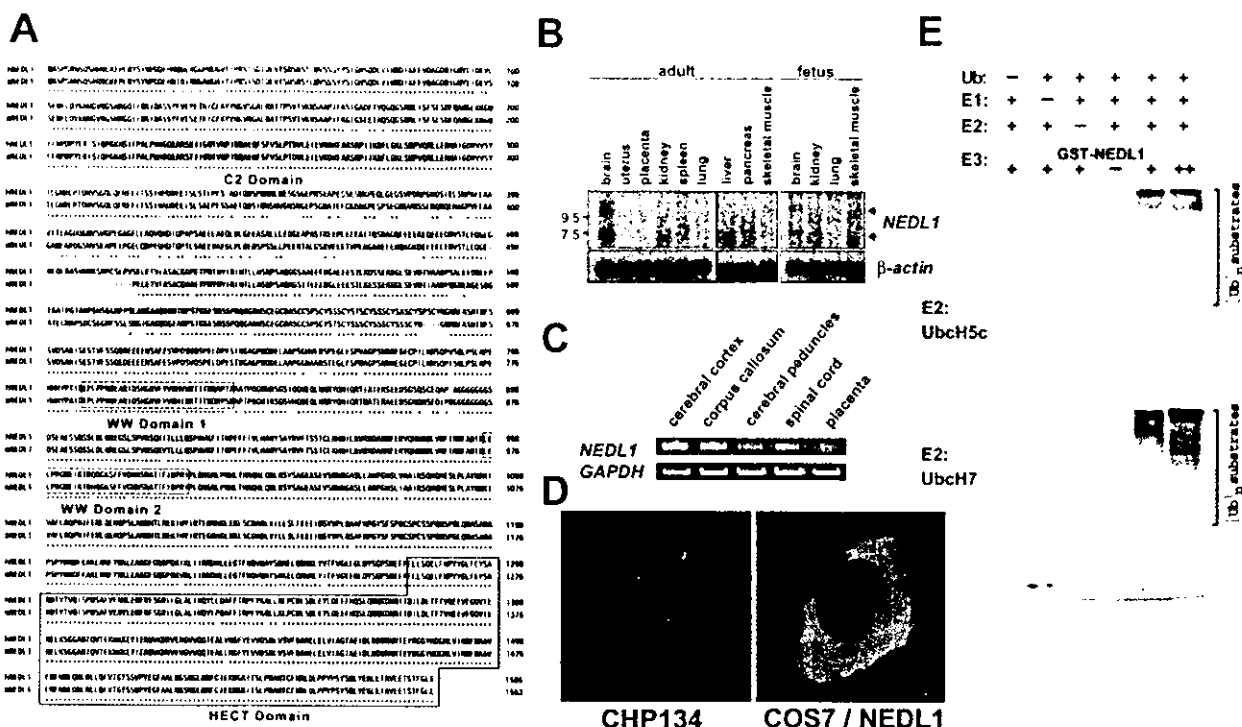


FIG. 1. Amino acid sequence, brain-specific expression, and subcellular localization of NEDL1 E3. *A*, alignment of conserved amino acid sequences of human NEDL1 (*hNEDL1*) and its mouse homolog (*mNEDL1*). Numbers on the right indicate the number of residues to the initiator methionine. The C2 domain (shaded), two WW domains (dashed boxes), and the HECT domain (solid box) are indicated. *B*, brain-specific expression of *NEDL1* mRNA. Total RNAs derived from the indicated adult (left panel) and fetal (right panel) human tissues were analyzed by Northern blotting using a ³²P-labeled human *NEDL1* cDNA restriction fragment as a probe. Control hybridization with a human β -actin cDNA probe verified the equal amount of RNA loaded. *C*, expression of *NEDL1* in human brain subsections. Total RNA from the cerebral cortex, corpus callosum, cerebral peduncles, spinal cord, or placenta was subjected to RT-PCR using specific primers for *NEDL1* or glyceraldehyde-3-phosphate dehydrogenase (*GAPDH*). RT-PCR analysis for *NEDL1* in the placenta provided a negative control. Amplification of glyceraldehyde-3-phosphate dehydrogenase was used as an internal control. *D*, confocal microscopic images of human neuroblastoma CHP134 cells (left panel) and COS-7 cells transfected with an expression plasmid for NEDL1 (right panel). Cells were subjected to immunofluorescence analysis using rabbit anti-NEDL1 polyclonal antibody, followed by fluorescein isothiocyanate-conjugated anti-mouse IgG. *E*, *in vitro* ubiquitination assays showing that NEDL1 has a ubiquitin-protein ligase activity. The degree of ubiquitination was increased in an NEDL1-dependent manner. In this assay, yeast ubiquitin-activating enzyme (*E1*), bacterially expressed ubiquitin carrier protein (*E2*; UbcH5c or UbcH7), and bacterial lysates were incubated in the presence or absence of increasing amounts of glutathione *S*-transferase (*GST*)-NEDL1. Polyubiquitinated bacterial proteins appeared to migrate in a high molecular mass complex. *Ub*, ubiquitin.

expression was also weakly detected in adult kidney, where the size of the expressed transcript appeared to be <7 kb. Expression of *NEDL1* in specific regions of the nervous system was further confirmed in the cerebral cortex, corpus callosum, cerebral peduncles, and spinal cord by RT-PCR (Fig. 1C). Thus, NEDL1 is a novel HECT-type E3 preferentially expressed in neuronal tissues, including the spinal cord. Using a specific anti-NEDL1 polyclonal antibody that we generated, we localized NEDL1 primarily to the cytoplasm in both intact human neuroblastoma CHP134 cells and COS-7 cells transiently expressing NEDL1 (Fig. 1D). The *in vitro* system containing UbcH5c or UbcH7 demonstrated that NEDL1 has a ubiquitin-protein ligase activity (Fig. 1E).

NEDL1 Physically Interacts with TRAP- δ and Mutant SOD1—We then sought protein-binding partners of NEDL1 by yeast two-hybrid screening using the region including two WW protein interaction domains (amino acids 757–1114) as bait. Of 96 positive clones subjected to DNA sequencing, one was a full-length cDNA for TRAP- δ ; this was of considerable interest, as TRAP- δ was previously reported to bind mutant (G85R and G93A), but not wild-type, SOD1 (9). TRAP- δ is a protein component of the translocon in the ER membrane (10). We therefore examined the interaction among NEDL1, TRAP- δ , and SOD1 by an immunoprecipitation assay after cotransfecting the corresponding expression constructs into COS-7 cells. As

shown in Fig. 2 (A and B), NEDL1 was physically associated with both exogenous and endogenous TRAP- δ probably through the region of two WW domains, as originally suggested by the result of two-hybrid screening. Surprisingly, NEDL1 bound to mutant (but not wild-type) SOD1 (Fig. 2C). Furthermore, the degree of binding between NEDL1 and different mutant SOD1 proteins was roughly proportionate to the rapidity of progression (time from clinical onset to death) of the associated FALS phenotype (17–23). For example, two mutant SOD1 proteins associated with an extremely rapid clinical course (C6F and A4V) interacted very strongly with NEDL1. By contrast, the binding of NEDL1 to other mutants was less striking and decreased proportionately to the falloff of disease severity corresponding to those mutants. Of further interest, like the NEDL1-mutant SOD1 interaction, the binding intensity between TRAP- δ and mutant SOD1 was also dependent on the disease severity (Fig. 2D). These observations suggest that NEDL1 and TRAP- δ are normally associated with each other, but that misfolded mutant SOD1 makes a complex with them. Such a complex is not formed with wild-type SOD1. The experiments using the *in vitro* translated proteins suggested that association of mutant SOD1 and TRAP- δ was direct (data not shown). It therefore appears that mutant SOD1 forms tightly bound protein complexes with NEDL1 and TRAP- δ and that the tightness of binding in the complex is determined in part by

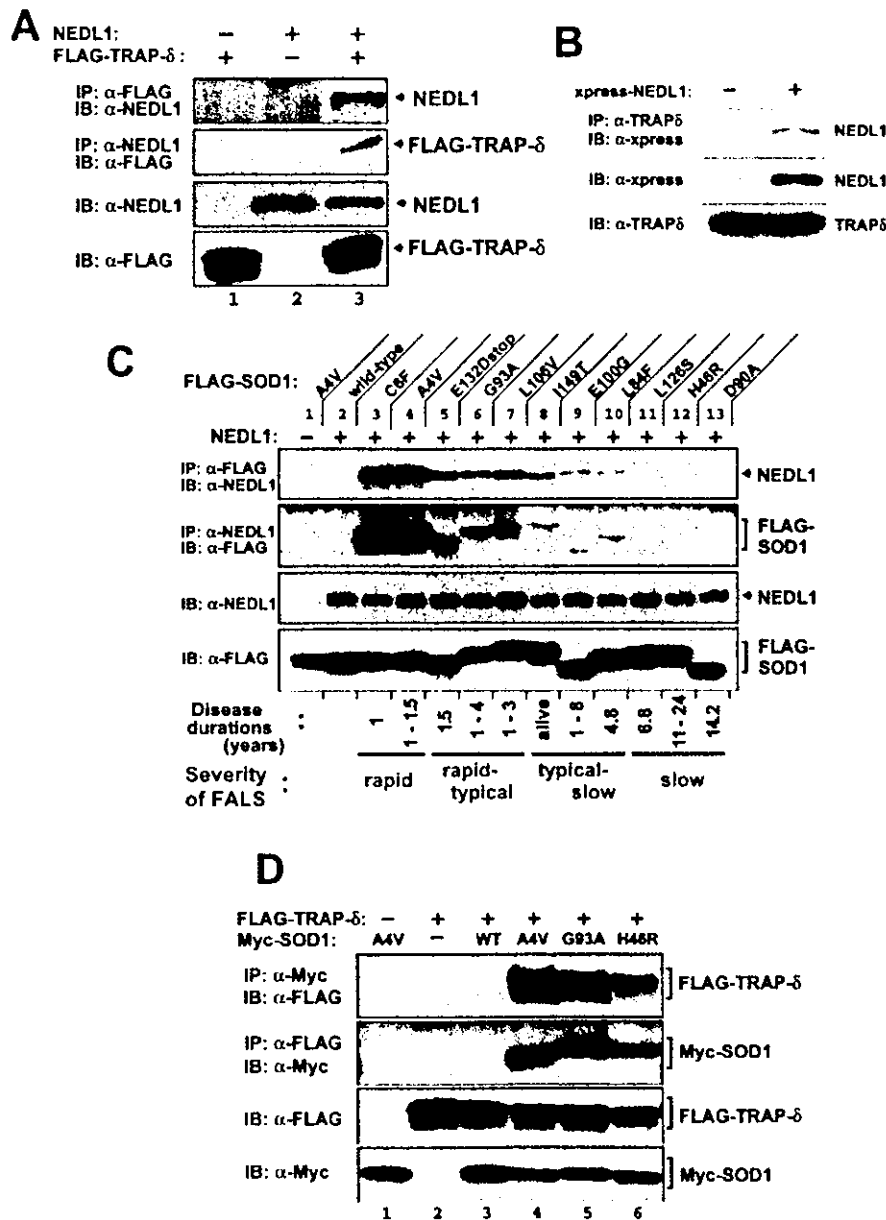


FIG. 2. NEDL1 interacts with TRAP- δ and FALS-associated mutant forms of SOD1, but not with wild-type SOD1. *A*, NEDL1 interacts with TRAP- δ . COS-7 cells were cotransfected with the indicated expression plasmids, and whole cell lysates were immunoprecipitated (IP) with anti-FLAG (*first panel*) or anti-NEDL1 (*second panel*) antibody. Immunoprecipitates were analyzed by immunoblotting (IB) using the indicated antibodies. Whole cell lysates were analyzed for expression levels of each protein by immunoblot analysis (*third and fourth panels*). Detection was performed with horseradish peroxidase-conjugated secondary antibodies. *B*, NEDL1 also binds to endogenous TRAP- δ . *C*, interaction between NEDL1 and mutant SOD1. Whole cell lysates from COS-7 cells overexpressing NEDL1 and one of the FLAG-tagged SOD1 mutants or wild-type SOD1 were immunoprecipitated with anti-FLAG (*first panel*) or anti-NEDL1 (*second panel*) antibody and then immunoblotted with anti-NEDL1 or anti-FLAG antibody, respectively. The expression of NEDL1 or FLAG-tagged SOD1 mutants was analyzed by immunoblotting using anti-NEDL1 (*third panel*) or anti-FLAG (*fourth panel*) antibody, respectively. Patients carrying the SOD1(C6F) and SOD1(A4V) mutations have a rapid clinical course, whereas mutant SOD1(L126S), SOD1(H46R), or SOD1(D90A) is associated with a slow clinical course. *D*, interaction of TRAP- δ with mutant SOD1. COS-7 cells were transiently cotransfected with the expression plasmid for FLAG-tagged TRAP- δ and the expression plasmid encoding one of the Myc-tagged SOD1 mutants or wild-type (WT) SOD1. Whole cell lysates were immunoprecipitated with anti-Myc (*first panel*) or anti-FLAG (*second panel*) antibody, followed by immunoblotting with anti-FLAG or anti-Myc antibody, respectively. The levels of overexpression of FLAG-tagged TRAP- δ (*third panel*) and Myc-tagged SOD1 (*fourth panel*) were analyzed by immunoblotting using anti-FLAG and anti-Myc antibodies, respectively.

properties of the mutant enzyme that also modulate disease severity of the resulting ALS phenotype. Such complexes do not form in cells with wild-type SOD1.

Determination of the Interaction Domains—We next examined the domains of NEDL1 required for formation of the SOD1-NEDL1-TRAP- δ complex. We generated various con-

structs of NEDL1 with deletions of each domain. Fig. 3 shows the results of immunoprecipitation assay for the association between deletion mutants of NEDL1 and mutant SOD1(G93A). Mutant SOD1 bound weakly to NEDL1 lacking WW domain-1 (Fig. 3A), suggesting that WW domain-1 and its surrounding portion are the region involved in their interaction. Immuno-

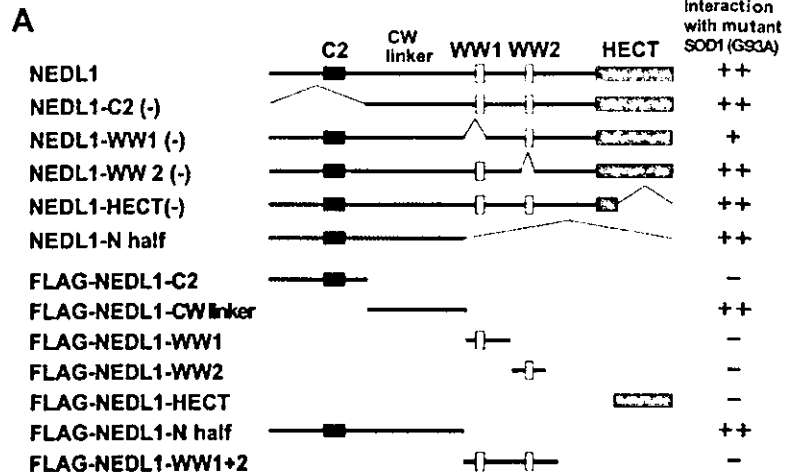
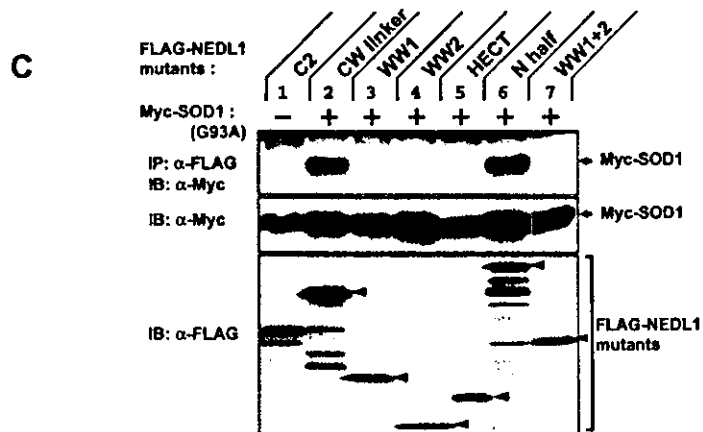
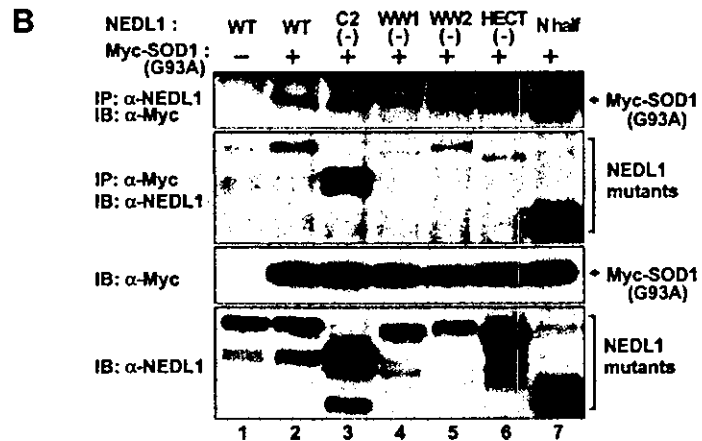


FIG. 3. The region of NEDL1 between the C2 domain and WW domain-1 is required for interaction with mutant SOD1. *A*, schematic illustration of wild-type NEDL1 and a series of deletion mutants of NEDL1. *CW linker* indicates the region between the C2 domain and WW domain-1 (*WW1*). *B* and *C*, immunoprecipitation and immunoblot analyses. In *B*, Myc-tagged mutant SOD1(G93A) was overexpressed together with wild-type (*WT*) NEDL1 or the indicated deletion mutants of NEDL1 in COS-7 cells. Whole cell lysates were immunoprecipitated (*IP*) with anti-NEDL1 (*first panel*) or anti-Myc (*second panel*) antibody, followed by immunoblotting (*IB*) with anti-Myc or anti-NEDL1 antibody, respectively. The expression levels of each protein were analyzed by immunoblotting using the indicated antibodies (*third and fourth panels*). In *C*, whole cell lysates were immunoprecipitated with anti-FLAG antibody and then immunoblotted with anti-Myc antibody (*upper panel*). Whole lysates were also analyzed by Western blotting for each protein (*middle and lower panels*).



precipitation analysis using the specific regions of NEDL1 clearly showed that the region between the C2 domain and WW domain-1 (*CW linker* region) is necessary for binding to mutant SOD1(G93A). Mutant SOD1(A4V) was also associated with NEDL1 through the same region, and TRAP-δ bound to the two WW domains of NEDL1 (data not shown).

NEDL1 Ubiquitinates Mutant SOD1 for Degradation Depending on the Disease Severity of FALS—Because NEDL1 is an E3, we next tested whether it ubiquitinates TRAP-δ and mutant SOD1 for degradation. As shown in Fig. 4A, NEDL1 clearly ubiquitinated mutant SOD1(A4V), but not TRAP-δ

(data not shown). Furthermore, the degree of ubiquitination of mutant SOD1 by NEDL1 was dependent on the disease severity of FALS (A4V > G93A > H46R) (Fig. 4A). Fig. 4B shows the time course of degradation of wild-type and mutant SOD1 in the presence or absence of NEDL1. As reported previously (46), mutant SOD1 was degraded more rapidly than wild-type SOD1. NEDL1 did not affect wild-type SOD1 degradation. As expected from the co-immunoprecipitation and ubiquitination analyses, degradation of mutant SOD1 was stimulated by NEDL1 proportionately to the disease severity of FALS caused by the particular SOD1 mutant (A4V > G93A > H46R ≅

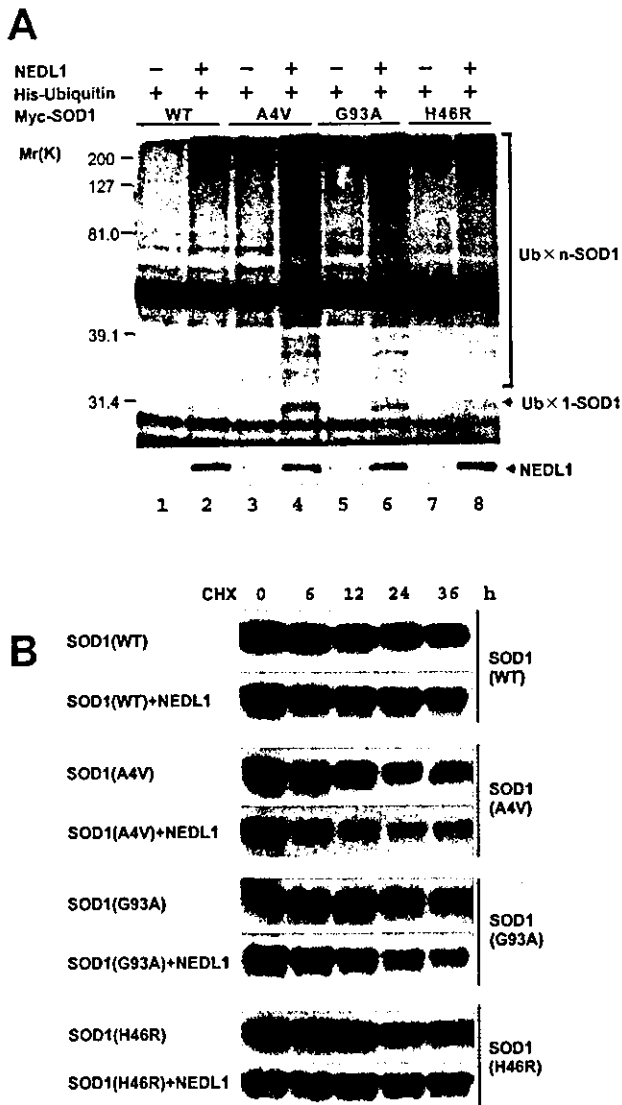


FIG. 4. NEDL1-dependent ubiquitination and degradation of mutant forms of SOD1 correlate broadly with their respective clinical phenotypes. **A**, NEDL1 ubiquitinates mutant SOD1 in a mutant type-dependent manner. COS-7 cells were transiently cotransfected with the indicated expression plasmids. Whole cell lysates from transfected COS-7 cells were immunoprecipitated with anti-Myc antibody, and immunoprecipitates were analyzed by Western blotting with anti-ubiquitin (Ub) antibody (upper panel). The bracket indicates slowly migrating ubiquitinated forms of SOD1. Whole cell lysates were analyzed by immunoblotting with anti-NEDL1 antibody to confirm the expression of transfected NEDL1 (lower panel). The running positions of molecular weight markers are indicated on the left. **B**, half-lives of wild-type (WT) and mutant SOD1 proteins in the presence or absence of NEDL1. Cell lysates were harvested from Neuro2a cells transfected with SOD1 alone or with SOD1 plus NEDL1 at different time points as indicated after the addition of cycloheximide (CHX; final concentration of 50 μ g/ml) and were analyzed for SOD1 protein levels by Western blotting with anti-FLAG antibody. In the presence of NEDL1, the half-lives of various mutant SOD1 proteins were reduced also roughly dependent on the disease severity of FALS (A4V > G93A > H46R).

wild-type). Thus, NEDL1 targeted mutant SOD1 for ubiquitin-mediated degradation in the cell in parallel with the binding intensity.

Immunohistochemistry—One of the characteristic cytopathological changes of mutant SOD1-linked FALS is the formation of neuronal Lewy body-like hyaline inclusions (LBHIs) that contain aggregates of SOD1 and ubiquitin (24). We therefore

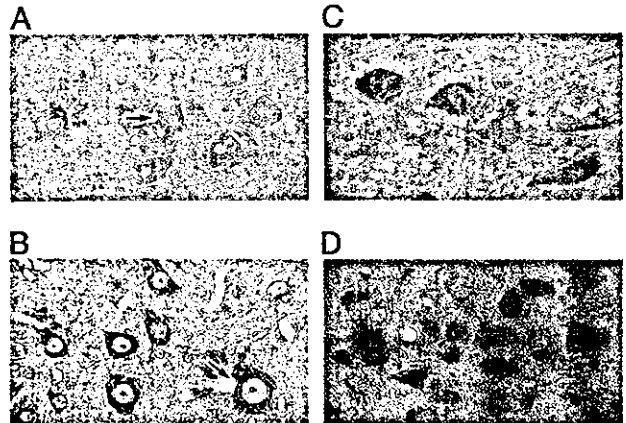


FIG. 5. NEDL1 immunohistochemical analyses. **A**, immunohistochemical analysis of NEDL1 in normal human spinal cord. NEDL1-positive anterior horn cells are evident (arrow), although the immunoreactivity for NEDL1 is somewhat faint. There was no counterstaining. Magnification $\times 520$. **B**, NEDL1 immunohistochemistry in normal mouse spinal cord. Normal anterior horn cells are positive for NEDL1 (arrow). The section was counterstained with hematoxylin. Magnification $\times 750$. **C**, immunostaining for NEDL1 in spinal cord LBHIs from an FALS patient with a frameshift 126 mutation in the SOD1 gene. The NEDL1-positive reaction products were mostly restricted to the cores of the core and halo-type LBHIs (arrowheads). In the LBHI-bearing neurons and residual neurons, the antibody to NEDL1 also stained the neuronal cell body. There was no counterstaining. Magnification $\times 540$. **D**, NEDL1 immunostaining in a spinal cord LBHI from an SOD1(H46R) transgenic mouse. An ill defined LBHI in the SOD1(H46R) transgenic mouse was positive for NEDL1; this ill defined LBHI shows a diffuse staining pattern (arrowhead). The staining intensity in the residual neurons stained by anti-NEDL1 antibody varied from neuron to neuron. The section was counterstained with hematoxylin. Magnification $\times 770$.

performed immunostaining to determine whether the NEDL1 protein is included within the LBHIs of the spinal cord motor neurons obtained from two siblings with FALS caused by frameshift 126 mutation of SOD1 (11, 12). One case had neuropathological findings compatible with FALS with posterior column involvement, whereas the other had multisystem degeneration in addition to motor neuron disturbance. We also performed NEDL1 immunostaining in specimens obtained from mutant SOD1(H46R) transgenic mice at 180 days, by which time they show clinical motor signs in the hind limbs (13). The specificity of the NEDL1 staining was confirmed by pretreating the specimens with an excess of NEDL1 antigen. NEDL1 immunoreactivity in the spinal cords of the human control cases was identical to that of normal mice: immunoreactivity was identified predominantly in the cytoplasm of the neurons of the spinal cords (Fig. 5, A and B). The LBHIs in the anterior horn cells of two FALS patients and transgenic mice showed equivalent immunoreactivity for NEDL1. Although the intensity of NEDL1 immunoreactivity in neuronal LBHIs varied, most of the LBHIs were immunoreactive for NEDL1 (Fig. 5, C and D). The reaction products were generally restricted to the cores of the core and halo-type LBHIs that showed eosinophilic cores with pale peripheral halos upon hematoxylin and eosin staining (Fig. 5C); by contrast, immunopositive NEDL1 in ill defined LBHIs was distributed throughout the inclusions (Fig. 5D). NEDL1 immunoreactivity in the residual neurons in humans and mice was identified primarily in cell bodies. Thus, NEDL1 immunostaining was clearly positive in the FALS-related LBHIs that were also positive for ubiquitin and SOD1 (data not shown).

NEDL1 Targets Dishevelled-1 for Ubiquitin-mediated Protein Degradation—We next hypothesized that the physiological function of NEDL1 to mediate ubiquitination is interfered with

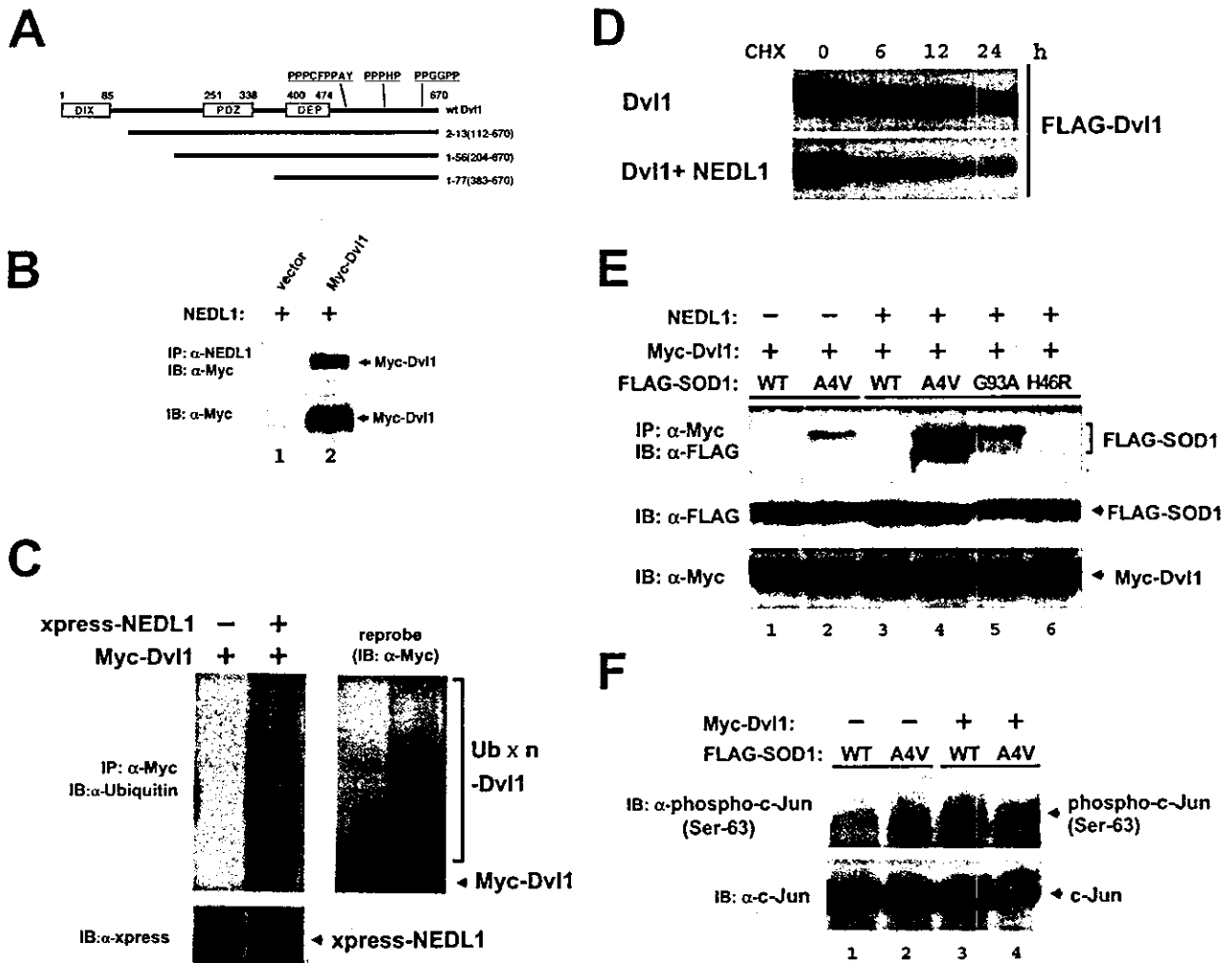


FIG. 6. Dvl1 is a substrate of NEDL1, and its functions are disturbed by mutant SOD1(A4V). *A*, schematic illustration of full-length Dvl1 and three clones obtained by yeast two-hybrid screening. Human Dvl1 consists of 670 amino acids and contains three conserved domains, including the DIX, PDZ, and DEP domains. Between the DEP domain and the C-terminal end, there are three proline-rich clusters, which might act as WW domain recognition sites. All three clones (clones 2–13, 1–56, 1–77) contain the DEP domain and these clusters. *B*, NEDL1 interacts with Dvl1. Myc-tagged Dvl1 was overexpressed together with NEDL1 in Neuro2a cells. Whole cell lysates were immunoprecipitated (IP) with anti-NEDL1 antibody, followed by immunoblotting (IB) with anti-Myc antibody (upper panel). The expression levels of Myc-tagged Dvl1 were analyzed by immunoblotting using anti-Myc antibody (lower panel). *C*, NEDL1 ubiquitinates Dvl1 in Neuro2a cells. The cells were transiently transfected with the indicated expression plasmids along with the ubiquitin expression plasmid in the presence or absence of the expression plasmid for XPRESS-tagged NEDL1. Whole cell lysates were immunoprecipitated with anti-Myc antibody and then immunoblotted with anti-ubiquitin antibody (left panel). The ladder of bands denoted by the bracket appeared to be ubiquitinated Dvl1. The expression of XPRESS-NEDL1 was analyzed by immunoblotting using anti-XPRESS antibody. The membrane was reprobbed with anti-Myc antibody (right panel). *D*, Dvl1 is degraded by NEDL1. Neuro2a cells were transfected with the expression plasmid for FLAG-tagged Dvl1 with or without the NEDL1 expression plasmid. Transfected cells were harvested at different time points as indicated after the addition of cycloheximide (CHX; final concentration of 50 μg/ml), and Dvl1 protein levels were analyzed by Western blotting with anti-FLAG antibody. In the presence of NEDL1, the half-lives of FLAG-Dvl1 were significantly reduced. *E*, Dvl1 binds to mutant SOD1(A4V), and the degree of its binding is enhanced in the presence of NEDL1. Whole cell lysates prepared from COS-7 cells transfected with the indicated combinations of expression plasmids were subjected to immunoprecipitation and Western analyses as indicated. *F*, c-Jun phosphorylation by overexpression of Dvl1 is suppressed upon coexpression of mutant SOD1(A4V). Whole cell lysates from COS-7 cells transfected with the indicated combinations of expression plasmids were subjected to Western blotting with antibody against the phosphorylated form of c-Jun (upper panel) or with anti-c-Jun antibody (lower panel). wt/WT, wild-type.

by mutant SOD1. To test this hypothesis, we again performed yeast two-hybrid screening to obtain NEDL1-interacting molecules using the large region of NEDL1 (amino acids 382–1448) as bait. Of 396 His and β-galactosidase double-positive clones, 282 clones were subjected to DNA sequencing, and we identified Dvl1 (three clones). Human Dvl1 is a 670-amino acid protein with three conserved domains: a DIX domain, which is required for canonical Wnt/T-cell factor signaling; a PDZ domain, which is a target of both Stbm and casein kinase I binding; and a DEP domain, which is responsible for Dvl membrane localization during planar cell polarity signaling (25–27). Between the DEP domain and C-terminal end, there are three

proline-rich clusters unique to mammalian Dvl1, which presumably act as the WW domain recognition sites. All three clones (clones 2–13, 1–56, and 1–77) contain the DEP domain and proline-rich clusters, suggesting that NEDL1 interacted with Dvl1 in the C-terminal half (Fig. 6A). In Neuro2a cells, NEDL1 co-immunoprecipitated with Dvl1 (Fig. 6B) and ubiquitinated it for degradation (Fig. 6, C and D). Thus, Dvl1 may be one of the physiological targets of NEDL1 E3. As recent studies strongly suggest that the cytotoxicity of SOD1 mutants is responsible for their aggregate properties, incorporating other proteins essential for cells into their aggregates (28), we examined the association between mutant SOD1 and Dvl1,

both of which interact with NEDL1. Of interest, Dvl1 bound to mutant SOD1(A4V), and complex formation was increased in the presence of NEDL1 roughly proportionately to the disease severity of FALS caused by the particular SOD1 mutant (Fig. 6E). Dvl1 is known to transduce not only the Wnt/ β -catenin/T-cell factor pathway, but also the JNK/c-Jun pathway (27). Therefore, we next examined whether the Dvl1-induced phosphorylation of c-Jun at Ser⁶³ was affected by the tight complex formation induced by inclusion of mutant SOD1. As shown in Fig. 6F, c-Jun phosphorylation induced by overexpression of Dvl1 was significantly suppressed by coexpression with mutant SOD1(A4V) in COS-7 cells.

DISCUSSION

Our present results demonstrate that a novel HECT-type NEDL1 E3, which is preferentially expressed in neuronal tissues, specifically targets mutant forms of SOD1 for ubiquitination-mediated protein degradation. NEDL1 is also associated with TRAP- δ localized at the ER translocon. The TRAP complex has recently been shown to facilitate the initiation of protein translocation in a substrate-specific manner (29). The NEDL1-TRAP- δ complex recognizes mutant (but not wild-type) SOD1, with a binding intensity that broadly parallels the disease severity of FALS. NEDL1 immunoreactivity was detected in the FALS-related LBHIs in the spinal cord ventral horn motor neurons, suggesting that, although mutant SOD1 is ubiquitinated for degradation by NEDL1, the mutant SOD1-NEDL1-TRAP- δ complex aggregates within the LBHIs. It is also conceivable that fragmentation of the Golgi apparatus reported in ALS patients and transgenic mice might be related to this aggregation (30, 31). These findings suggest possible hypotheses for the role of NEDL1 in the pathogenesis of FALS: 1) NEDL1, alone or with TRAP- δ , ubiquitinates and aggregates mutant SOD1, thereby decreasing the function of mutant SOD1; 2) NEDL1 and TRAP- δ form aggregates with mutant SOD1 that induce fragmentation of the Golgi apparatus, leading to neuronal apoptosis; 3) formation of these aggregates causes dysfunction of NEDL1 and/or TRAP- δ , and this, in turn, induces disturbances that ultimately cause motor neuron death; and 4) the mutant SOD1-NEDL1-TRAP- δ aggregates trap and inactivate unknown factor(s) such as molecular chaperones whose normal function is important for motor neuron viability.

To further understand the role of NEDL1 in motor neuron death, we searched for the physiological targets of NEDL1 and identified Dvl1. As expected, Dvl1 is ubiquitinated for degradation by NEDL1. Surprisingly, however, Dvl1 also interacts with mutant SOD1 in the presence of NEDL1 roughly proportionately to the disease severity of FALS caused by the particular SOD1 mutant. Dvl1, an essential multimodule signal transducer localized in the cellular cytosol and cytoskeleton, mediates planar cell polarity signaling as well as canonical Wnt/ β -catenin signaling (27, 32). In mammals, three Dvl family members have so far been reported, and the level of Dvl1 expression is high in neuronal tissues (33). As far as we know, NEDL1 is the first E3 for Dvl1, interacting with the C-terminal region containing three proline-rich clusters. A recent report suggests that Dvl1 regulates microtubule stability through inhibition of glycogen synthase kinase-3 β (34). Because cytoskeletal abnormalities have been reported in ALS motor neurons (35), it is possible that the effect of mutant SOD1 on NEDL1-mediated Dvl1 degradation is involved in the motor neuron death. Furthermore, Dvl1 is abundant in the postsynaptic membrane region at the neuromuscular junction (36) that is reported to be involved in several neurodegenerative disorders (37, 38). Of interest, *Dvl1* is mapped to chromosome 1p36, which is a commonly deleted region in many human cancers,

including neuroblastoma (39). As NEDL1 is highly expressed in neuroblastomas with favorable prognosis, which have a tendency to differentiate and/or regress, NEDL1 may be involved in the regulation of neuronal differentiation and survival possibly by controlling Dvl1.

NEDL1, TRAP- δ , mutant SOD1, and Dvl1 appear to form a complex roughly proportionately to the disease severity of FALS caused by the particular SOD1 mutant. Our present observations strongly suggest that NEDL1 may be a quality control E3 recognizing misfolded mutant SOD1 (40). The association between mutant SOD1 and NEDL1 may induce the conformational change in the NEDL1 protein to increase the binding intensity with other physiological targets such as TRAP- δ (not ubiquitinated) and Dvl1 (ubiquitinated). This may lead to tight complex formation especially when the proteasome activity is impaired. It has been reported that the expression and function of proteasomes decrease with age in the spinal cord (7). Okado-Matsumoto and Fridovich (41) have also found that complex formation between mutant SOD1 and heat shock proteins leads to protein aggregates. Because our data show that the ER translocon component TRAP- δ is involved, aggregate formation may occur at the sites of the ER or Golgi apparatus or even at other cellular sites. The complex formation including NEDL1 and mutant SOD1 may conversely affect the physiological function of NEDL1, as demonstrated by a decrease in Dvl1-induced phosphorylation of c-Jun.

Recently, the RING finger-type E3 Dorfin has been reported to ubiquitinate mutant SOD1 for degradation (42). However, NEDL1 and Dorfin appear to be different in several aspects. First, NEDL1 is expressed specifically in neuronal tissues, including the spinal cord, whereas Dorfin is ubiquitously expressed in most human tissues. Second, both interaction between NEDL1 and mutant SOD1 and ubiquitination of the latter by NEDL1 roughly parallel the disease severity caused by the particular SOD1 mutant, whereas Dorfin similarly ubiquitinates mutant forms of SOD1. In addition, we have identified Dvl1 and TRAP- δ as cellular target proteins of NEDL1, whereas the physiological targets of Dorfin have never been reported. It is probable that there are some other E3 ligases targeting mutant SOD1. However, the molecular characteristics, including tissue-specific expression, subcellular localization, and age-dependent expression, might be important in the development of the FALS phenotype.

In conclusion, we have identified a novel neuronal E3 (NEDL1) that interacts with TRAP- δ and also binds to and ubiquitinates Dvl1 for degradation. Strikingly, NEDL1 targets and ubiquitinates mutant (but not wild-type) SOD1 for degradation. NEDL1 may normally function in the quality control of cellular proteins by eliminating misfolded proteins such as mutant SOD1, possibly via a mechanism analogous to that of ER-associated degradation (43–45). NEDL1 appears to complex tightly with mutant SOD1, Dvl1, and TRAP- δ , forming aggregates with species of mutant SOD1 that have escaped ubiquitin-mediated degradation. The NEDL1 function that affects the activities of the target proteins may also be modulated by mutant SOD1. All of these might contribute to the pathogenesis of FALS; further elucidation of the molecular mechanism of formation of this complex and its pathogenicity may provide insights into motor neuron death in ALS as well as possible new therapeutic strategies for ALS.

Acknowledgments—We thank Robert H. Brown, Jr. (Harvard Medical School) for critical comments and reading the manuscript. We also thank M. Ohira and Y. Nakamura for helping with cDNA cloning and sequencing; K. Watanabe and M. Suzuki for making plasmid constructs; M. Nagai and M. Kato for helping with immunohistochemical studies; S. Hatakeyama, M. Matsumoto, and K. Nakayama